Activation of *Shaker* Potassium Channels
II. Kinetics of the V2 Mutant Channel

N.E. Schoppa and F.J. Sigworth

From the Department of Cellular and Molecular Physiology, Yale University School of Medicine, New Haven, Connecticut 06520

ABSTRACT This second of three papers, in which we functionally characterize activation gating in *Shaker* potassium channels, focuses on the properties of a mutant channel (called V2), in which the leucine at position 382 (in the *Shaker* B sequence) is mutated to valine. The general properties of V2's ionic and gating currents are consistent with changes in late gating transitions, in particular, with V2 disrupting the positively cooperative gating process of the normally activating wild type (WT) channel. An analysis of forward and backward rate constants, analogous to that used for WT in the previous paper, indicates that V2 causes little change in the rates for most of the transitions in the activation path, but causes large changes in the backward rates of the final two transitions. Single channel data indicate that the V2 mutation causes moderate changes in the rates of transitions to states that are not in the activation path, but little change in the rates from these states. V2's data also yield insights into the general properties of the activation gating process that could not be readily obtained from the WT channel, including evidence that intermediate transitions have rapid backward rates, and an estimate of a total charge 2 e_0 for the final two transitions. Taken together, these data will help constrain an activation gating model in the third paper of this series, while also providing an explanation for V2's effects.

KEY WORDS: ion channel • gating current • single-channel current • patch clamp • kinetic model

INTRODUCTION

The S4-S5 region of many voltage-gated channels contains a leucine heptad repeat motif (McCormack et al., 1989) that, in the *Shaker* B amino acid sequence, spans residues 375–403. A possible role of this motif in the *Shaker* channel activation process was suggested by the work of McCormack et al. (1991) in which the five leucines were individually substituted by other hydrophobic residues. Substitutions of the first two leucines (L1 and L2) by valine were seen to produce positive shifts of the midpoint voltage of activation of 60 mV or more and reduce the voltage sensitivity. Substitution of alanine for L1 has a similar effect (Lopez et al., 1991), as does the substitution of phenylalanine in the L1 position in Domain 1 of the rat brain II sodium channel (Auld et al., 1990).

This paper concerns a mutation in which L2 is substituted by valine, referred to here as the V2 mutation. Despite the reduced voltage sensitivity of the V2 channel, a comparison of gating currents in noninactivating wild-type (WT)[1] and V2 channels in a previous study showed no change in the total charge movement per channel (Schoppa et al., 1992). To interpret these effects, we previously fitted the equilibrium voltage dependence of channel opening and charge movement to a model similar to:

$$(S_0 \underset{(2.55\ e_0)}{\overset{k_1}{\rightleftharpoons}} S_1)_4 \underset{(2.1\ e_0)}{\overset{k_2}{\rightleftharpoons}} O \quad .$$

(SCHEME I)

This model, which invokes the tetrameric structure of *Shaker* channels (MacKinnon, 1991; Kavanaugh et al., 1992; Li et al., 1994), has the channel open after each of four subunits undergoes one transition (from S_0 to S_1) and one additional concerted conformational change. In the context of this model, V2 causes a 70-mV positive shift in the midpoint voltage for the equilibrium constant k_2, but causes a negligible (5-mV) shift in the midpoint voltage of k_1 (Schoppa et al., 1992). The strongly shifted midpoint voltage of k_2 allows the V2 channel to open only at depolarized voltages and confers the weak voltage dependence of k_2 on the channel open probability. Subsequent analysis of other point mutations of L2 has provided some information about changes in the local environment of that residue (McCormack et al., 1993; Sigworth, 1994; Holmgren et al., 1996) and a possible role of this residue in the inactivation process (Ayer and Sigworth, 1997).

While Scheme I provides a useful framework for considering V2's effects on equilibrium properties, it can-

Dr. Schoppa's present address is Vollum Institute, Oregon Health Sciences University L-474, Portland, OR 97201-3098.

Address correspondence to Fred J. Sigworth, Department of Cellular and Molecular Physiology, Yale University School of Medicine, 333 Cedar Street, New Haven, CT 06520. Fax: 203-785-4951; E-mail: fred.sigworth@yale.edu

[1]*Abbreviation used in this paper:* WT, wild type.

not describe *Shaker*'s activation kinetics. The scheme has the channel undergo only five transitions, which cannot produce a long enough delay to account for the channel activation time course (Zagotta et al., 1994*a*, 1994*b*; Schoppa and Sigworth, 1998*b*). Also, the model has only two different types of transitions, while *Shaker* channels have at least three distinct types of transitions that can be distinguished by their voltage dependences (Schoppa and Sigworth, 1998*a*).

In this paper, we extend the kinetic analysis of the *Shaker* channel to the effects of the V2 mutation. This characterization of V2 serves two purposes. First, it serves to further delineate the steps in channel activation that are affected by the structural changes caused by the mutation. Second, it can provide additional information about the channel activation process. Because the V2 mutation leaves the total gating charge unchanged, we will assume that its effects can be explained by changes in the free energy of conformational states of the protein, leaving unaffected the charge movements accompanying the transitions. Thus, we assume that the basic conformational changes that are involved in channel opening are preserved in V2. This view is supported by the qualitatively similar effects of four other amino acid substitutions at this position (McCormack et al., 1993; Sigworth, 1994), and by the similar voltage dependences seen in rate constants of WT and V2 channels, as will be shown here. From within this framework, the data obtained from V2 can provide some insights into the activation gating process that cannot be directly obtained from WT data. In the following paper (Schoppa and Sigworth, 1998*b*), these data will be used to help constrain a model of the activation process that accounts simultaneously for the properties of V2 and WT channels.

As in the study of the normally activating WT channel in the preceding paper, the V2 mutant channel that we study has its NH_2 terminus truncated to remove the fast inactivation process (Hoshi et al., 1990). It was characterized using patch-clamp measurements of macroscopic ionic and gating currents, and also single channel currents recorded from oocytes expressing the V2 channel. In this paper, we first consider the general effects of the V2 mutation on activation gating, and then present a detailed analysis of rate constants that parallels the analysis performed on WT in the previous paper.

METHODS

V2's macroscopic ionic and gating currents and single channel currents were measured in inside-out membrane patches from *Xenopus laevis* oocytes expressing the V2 channel, which in our experiments contains a deletion of residues 2–30 to remove N-type inactivation (Hoshi et al., 1990). The construction of the V2 *Shaker* 29-4 cDNA and in vitro synthesis of cRNA have been described previously (McCormack et al., 1991; Schoppa et al., 1992). The current recordings were made as described previously (Schoppa and Sigworth, 1998*a*), with some differences in procedures related to possible artifacts as described below.

Ion and Time Effects on V2's Macroscopic Currents

In our previous paper (Schoppa and Sigworth, 1998*a*), we reported that the substitution of cesium ions for potassium in the bath, done to facilitate the removal of ionic currents, caused small changes in WT's gating currents. A comparison of V2's gating currents recorded in different patches with bath Cs^+ or K^+ indicated that these currents are kinetically similar, and the *Q-V* relations that were derived from these two types of measurements are not distinguishable. Gating currents recorded in Cs^+ were thus used more extensively than was the case for WT experiments, and were used in the experiments shown in Figs. 4 *C* and 8.

Secondly, it was reported (Schoppa and Sigworth, 1998*a*) that WT's macroscopic ionic tail currents displayed a threefold slowing during the first several minutes of a given patch recording. However, for V2, the time-dependent changes in deactivation were much smaller: from <45 s after patch excision to ≥ 4 min later, ionic tail currents showed a nonsignificant slowing of only $15 \pm 11\%$ ($n = 3$). Therefore, in contrast to experiments with WT channels, V2 tail currents measured immediately after excision were not excluded from the analysis of the deactivation process. None of the other macroscopic gating properties showed time-dependent effects, as was also observed for WT channels in the previous study.

Heterogeneity in V2 Single-Channel Behavior

In recordings of single channel currents, one important consideration is the stationarity of the channel behavior, as inhomogeneous kinetics introduce spurious components into the closed and open dwell-time histograms. Here we describe that V2's single channels display two types of nonstationarities and discuss how each was taken into account in our analysis.

The first type of nonstationary behavior corresponds to obvious shifts in the voltage dependence of P_o that lasted for tens of minutes. In one single-channel patch recording that lasted 84 min, currents were measured at +7 mV during three different 2–3-min epochs at 10, 35, and 70 min after patch excision. Between the epochs, the mean P_o changed from 0.46 ± 0.14 (mean $\pm$ SD; $n = 151$ traces) to 0.20 ± 0.15 ($n = 86$) and back to 0.50 ± 0.16 ($n = 78$). The change was well described by a 20-mV shift in the voltage dependence of P_o, as well as in many kinetic parameters that were derived from the closed dwell-time histograms, the first latencies, and the ensemble average current taken from the data. A similar reversible switch from high to low P_o activity was observed in one other patch recording, with the P_o-*V* relations during the high and low P_o periods in this second patch recording being nearly superimposable with the P_o-*V* relations in the first patch recording. Also, in nine additional patch recordings in which P_o was relatively stable, the derived P_o-*V* relations clustered around the same two voltage ranges. These results would suggest that the observed changes in P_o did not arise from artifacts such as a change in the temperature of the bathing solution; we take this behavior instead as indicative of two gating modes.

To avoid the effects of these shifts in P_o, we ignored all low P_o-mode activity in the analysis. This approach was justified since the V2 channel apparently spends much more time in the high than in the low P_o mode. Of 11 single-channel patch recordings, two patches displayed both high and low P_o-mode activity, seven patches displayed only high P_o-mode activity, and only two patches displayed only low P_o-mode activity. In these 11 patches, high P_o-mode activity was displayed during 78% of the total 482 min of recording time. Additionally, an analysis of a variety of equilibrium and kinetic parameters indicated that V2 macro-

scopic currents were composed of the summed activity of a large number of mostly high P_o-mode channels. For example, the activation time constant τ_a derived from the rising phase of the macroscopic current was similar to the τ_a derived from the ensemble average of the high P_o-mode single channels but not that from low P_o-mode single-channel events.

V2's single channel activity, like WT's (Schoppa and Sigworth, 1998*a*), also showed a subconductance behavior, in which the channel occasionally shows a reduced current amplitude. This activity was accounted for by ending the analysis of a given single channel current trace at the point at which the currents appear to become smaller.

Evidence that our selection criteria did not significantly bias the analysis was obtained by considering the properties of the idealized single channel activity as contained in the event tables produced by the analysis program. For a channel with one open state, the form of the macroscopic tail current as a function of time τ should match the conditional probability of the channel being open at time $t + \tau$ given that the channel is open at t. In several patches, this conditional probability was computed within individual sweeps and averaged across sweeps; the resulting time course matched well the time course of macroscopic tail currents at the same voltage.

Slow Inactivation

Parameters of double-exponential fits to the slow inactivation phase of V2's currents were very similar to those of WT: at +67 mV, V2's current measured during 4-s pulses decayed with time constants of 76 ± 19 and 1,136 ± 250 ms ($n = 3$) with the fast component comprising 28 ± 17% of the total amplitude. Fits of exponentials to the ionic currents that are reported include a term reflecting the ~80-ms component of the slow inactivation process.

Characterization of Kinetics and Voltage Dependences

For characterization of the time course of channel activation, a single-exponential function with time constant τ and delay δ,

$$I(t) = I_{max}(1 - e^{-(t-\delta)/\tau}), \quad t > \delta, \tag{1}$$

was fitted to the time course of the current, starting at the time when the current has reached 50% of its final value I_{max}. It was shown in the preceding paper that, in the case of a sequential scheme with unidirectional transitions, δ provides a remarkably good estimate of the sum of the reciprocals of all of the rate constants, excluding the smallest one. Further, if one transition is rate limiting, its rate constant is well estimated by τ^{-1}; this result also holds for branched models. In some cases, when this function was fitted to activation time courses, we added a second exponential term with a longer time constant to account for a slow relaxation that is seen at depolarized voltages.

As before, we assume that rate constants have exponential voltage dependences of the form

$$\alpha_i(V) = \alpha_i(0)\, e^{q_{\alpha i} V/kT} \text{ and}$$

$$\beta_i(V) = \beta_i(0)\, e^{q_{\beta i} V/kT}, \tag{2}$$

where the partial charges $q_{\alpha i}$ and $q_{\beta i}$ are related to the gating charge movement z_i accompanying a transition from state $i - 1$ to state i according to

$$z_i = q_{\alpha i} - q_{\beta i}. \tag{3}$$

As a simple characterization of the equilibria of voltage-dependent processes, we use fits to a Boltzmann function,

$$b(V) = \frac{1}{1 + e^{-q_B(V - V_{1/2})/kT}}, \tag{4}$$

where q_B is the effective charge parameter.

Values of quantities are given as mean ± SEM unless otherwise noted.

RESULTS

General Properties of V2 Channels

Comparison of WT and V2's equilibrium properties. Fig. 1, *A* and *B* compares the voltage dependence of channel open probability P_o and the single-channel charge movement q in WT and V2 channels. As described previously (Schoppa et al., 1992), the V2 mutation causes a large positive shift in the voltage dependence of channel opening, and makes the P_o-V curve less steep. In fits of P_o-V relations obtained in several patches, values for the Boltzmann charge parameter ranged from 3 to 4 e_0 for WT, but from 1.5 to 2 e_0 for V2. For the q-V relation, V2 causes a large positive shift in the voltage dependence of part of the charge movement, and also apparently reduces the steepness of the q-V relation. A number of possible explanations exist for WT's steep voltage dependence of P_o and q (Bezanilla et al., 1994; Zagotta et al., 1994*a*); for example, there may be positive cooperativity introduced by a late gating transition that is very forward biased. V2 might lower the voltage sensitivity of P_o and q, if V2 alters the equilibrium of such a late gating transition.

In V2's q-V relation, there also appears to be an inflection near −10 mV. This is graphically illustrated in the plot of the derivative of V2's charge versus voltage in Fig. 1 *C*. The derivative plot has two peaks: the largest near −50 mV, which corresponds to the steepest portion of V2's q-V relation at negative voltages, and a second peak near +10 mV. These properties would be consistent with there being two distinct sets of transitions occurring over different voltage ranges. From the position of the inflection in the q-V relation (Fig. 1 *B*), which is near −13 mV, we can divide the charge movement into two parts, q_L and q_H, associated with the sets of transitions that occur at low and high voltages, respectively. A value of $q_H = 2.2 \pm 0.3$ e_0 ($n = 6$) is estimated for the amount of charge that is associated with the set of transitions that move at high voltages.

Comparison of WT and V2 channel opening and "on" gating current kinetics. V2's general effects on gating kinetics are illustrated in the time courses of the macroscopic ionic current and gating currents in Figs. 2 and 3. In a comparison of channel opening time courses (Fig. 2), V2 displays somewhat slower kinetics at both low and high voltages. The difference at lower voltages is re-

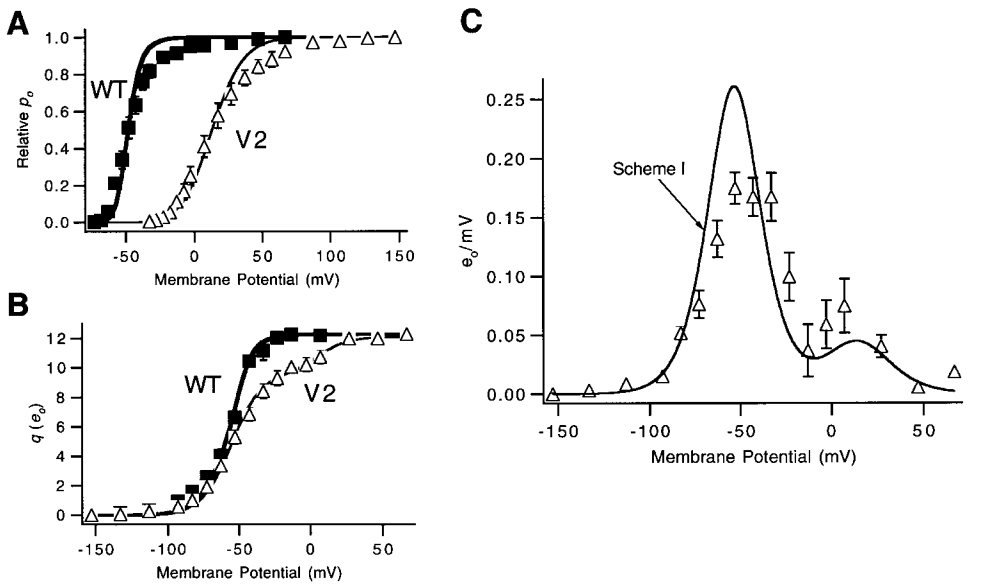

FIGURE 1. WT and V2's voltage dependence of charge movement and channel opening. (*A*) Voltage dependence of channel opening P_o for WT (■) and V2 (△). The P_o values were evaluated from macroscopic ionic currents as described in Fig. 1 of Schoppa and Sigworth (1998*a*) and were normalized to unity. Each value reflects one to nine experiments. Superimposed curves are fits of Scheme I to the averaged data with $V_{1/2}$ values for k_1 equal to −59 and −54 mV, and $V_{1/2}$ values for k_2 equal to −54 and +14 mV, for WT and V2 respectively. (*B*) Voltage dependence of charge movement for WT (■) and V2 (△) scaled to match the maximal single-channel charge movement, q_{max} = 12.3 e_0 (Schoppa et al., 1992). Each value reflects one to seven experiments. Superimposed curves are fits to Scheme I to the averaged WT and V2 data with parameter estimates given in *A*. (*C*) The derivative $\Delta q/\Delta V$ of V2's q-V relation was calculated from the difference in q measured between different voltages (in 10-mV increments, except 20-mV increments at $V \leq -93$ and $V > +7$ mV). Each value reflects measurements in four patches. Besides the main peak centered near −50 mV, a second smaller peak is seen at depolarized voltages near +10 mV. The smooth curve is the derivative of the simulated q-V curve shown in *B* for V2.

flected in the differences in the values for the activation time constant τ_a, with V2 displaying τ_a values that are as much as two to three times slower than WT (Fig. 2 *B*). The τ_a values are, however, very similar above +60 mV. Over the entire voltage range, the delay in the channel opening time course is roughly similar to WT's (Fig. 2 *C*).

Interpreting the ionic currents is complicated by the fact that at high voltages ($V \geq +67$ mV), *Shaker*'s channel opening time course has a slow component that reflects the kinetics of an alternate activation path, through the closed states C_i (Schoppa and Sigworth, 1998*a*). However, in fits of the sum of two exponentials to the channel opening time course at $V \geq +67$ mV, V2 causes no apparent effect on the time constant of the faster component (Fig. 2 *B*), which we take to be τ_a, reflecting the kinetics of the main activation path. It will be shown more explicitly below that the difference in the appearance of the currents at high voltages reflects a higher propensity for V2 to enter into the slow activation path.

The on gating current time courses of V2 (Fig. 3 *A*) are qualitatively similar to WT's. The similar time courses at many of the voltages are reflected in the similar values for the time constant τ_{on} of an exponential fitted to the decay of the on currents (Fig. 3 *B*). The similar gating current time courses at voltages above 0 mV, together with the discrepancies in WT and V2 channel opening time courses at the same voltages (Fig. 2 *A*), implies that V2 has little effect on early gating transitions, but an effect on late transitions. For a sequential gating mechanism, decreasing the rate of an early gating transition would slow both the ionic and gating current time courses, but a change in a late transition could slow channel opening without affecting the gating current.

Some moderate differences in the τ_{on} values are apparent at intermediate voltages, near −40 mV, where V2's on currents decay nearly twice as rapidly as WT's. This difference might be an indirect effect of V2's shifted voltage dependence of channel opening. It has been reported that WT's on currents at these voltages include a slow component that reflects the slow kinetics of channel opening (Bezanilla et al., 1994). Since V2 does not open at these voltages, this component would not be expected to appear in V2's currents (McCormack et al., 1994). Consistent with this simple interpretation, WT's on currents at −43 mV (Fig. 3 *C*) can be fitted by the sum of two exponentials with one component having a time constant (τ = 4.2 ± 0.5 ms; n = 4) that matches WT's activation time constant at this voltage (τ_a = 4.9 ± 0.9 ms; n = 5), and the other component having a time constant (τ = 1.2 ± 0.2 ms; n = 4) that matches the time constant of the single exponential fitted to V2 gating currents (τ = 1.2 ± 0.1 ms; n = 4).

In contrast to the modest effects on the on gating currents, V2 has a dramatic effect on the decay of the "off" gating currents. After moderate and large depolarizations, V2's gating currents decay very much more rapidly than WT's. To explain V2's faster off gating cur-

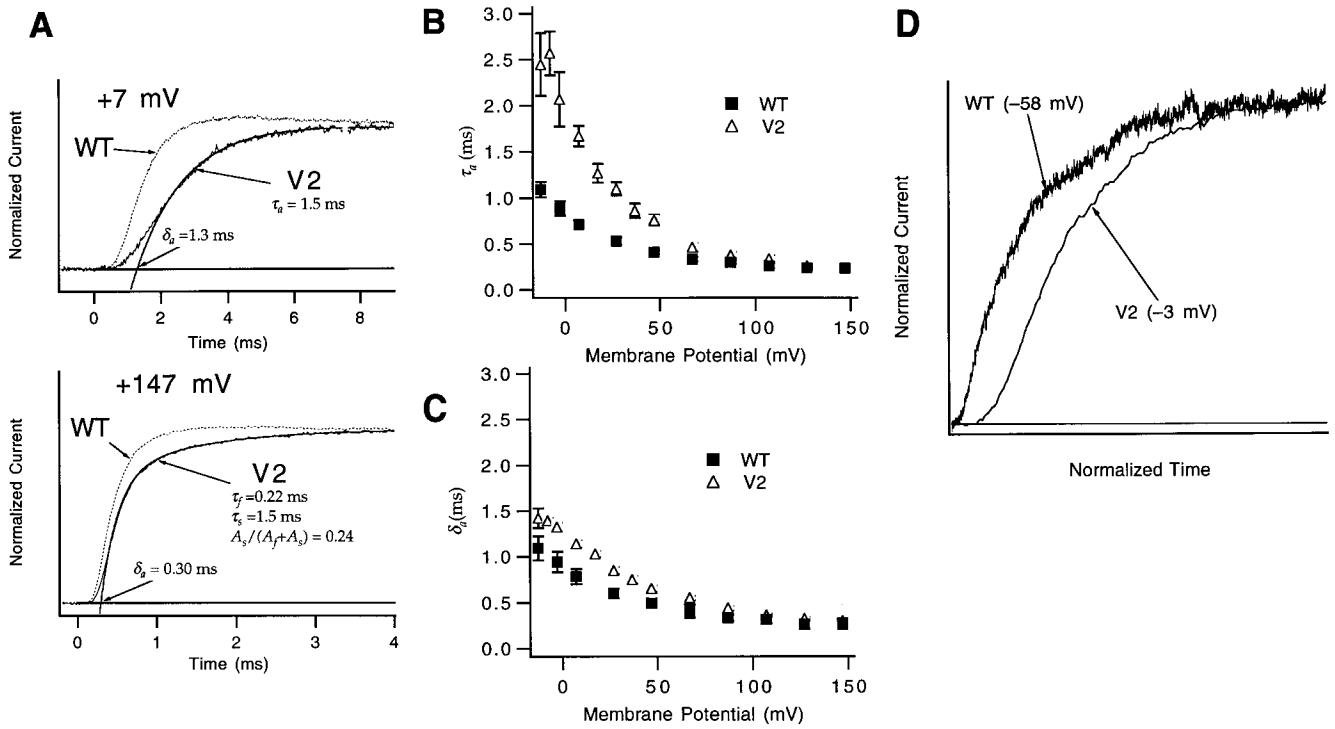

FIGURE 2. V2's effects on activation kinetics. (*A*) At both low and high voltages, V2 has slower channel opening kinetics, reflected here in a comparison of WT and V2 currents at +7 and +147 mV. Patches w312 and v096. V2's ionic current at +7 mV was fitted to a single exponential to estimate the activation time constant τ_a and an activation delay δ_a. The current at +147 mV was fitted to the sum of two exponentials, $I(t) = (A_f + A_s) - A_f e^{-(t-\delta_a)/\tau_a} + A_s e^{-(t-\delta_a)/\tau_s}$. The faster time constant is τ_a, which is taken to reflect the kinetics of the main activation path (Schoppa and Sigworth, 1998*a*). (*B*) The derived values for τ_a for V2 are larger than WT at $V < +67$ mV, but are similar at higher voltages. Individual values reflect two to seven experiments. Error bars are smaller than the symbols in many cases. (*C*) WT and V2 have similar, though not identical, values for the activation delay δ_a (from the same experiments as in *B*). (*D*) Comparison of the sigmoidicity of WT and V2 ionic currents at voltages where the two channels have $P_o \cong 0.2$. The current traces have normalized amplitudes and have their time axes scaled to yield the same rising phase kinetics of the current. Patches w312 and v142.

rents, we recognize first that WT's off currents after large, long depolarizations have a slow decay time course that reflects the slow return from the open state but a rapid decay time course after small or short depolarizations that fail to open the channel (Zagotta et al., 1994; Bezanilla et al., 1994). V2's faster off current after intermediate depolarizations (e.g., to −33 mV) could, then, just be due to the fact that V2 does not open at these voltages (Fig. 1 *A*). The faster off currents also seen after depolarizations that are large enough to open V2 channels ($V \geq -13$ mV) are to be expected since, as shown below, V2 dramatically speeds the deactivation time course.

Comparison of WT and V2 channel opening kinetics at equivalent P_o. A final general kinetic effect of the V2 mutation is illustrated in Fig. 2 *D*, where WT and V2 activation time courses are compared at voltages where P_o is similar for the two channels. The displayed currents are at −58 mV for WT and −3 mV for V2, where P_o is ~0.2 for the two channels. We follow the strategy used by Zagotta et al. (1994*a*) by normalizing the amplitude and the time course of the currents to make comparisons about the sigmoidicity of WT and V2 currents.

WT's activation time course is actually ~20-fold slower than V2's, but when the time scales have been adjusted to match the activation time constants τ_a, V2's activation time course is seen to be much more sigmoidal than WT's. One explanation for the slow rise and relatively small delay of WT currents is that there is positive cooperativity in the mechanism of activation at these voltages, arising from the presence of forward-biased late transitions (Zagotta et al., 1994*b*). The faster rise but approximately equal delay in V2 activation is consistent with unchanged early activation steps but a late transition that is less forward biased.

Assignment of Rate Constants from Macroscopic Currents

The preceding sections have outlined the general differences in activation gating for WT and V2 channels. We now consider the rates of individual V2 gating transitions. For this analysis, we use the same general frame-

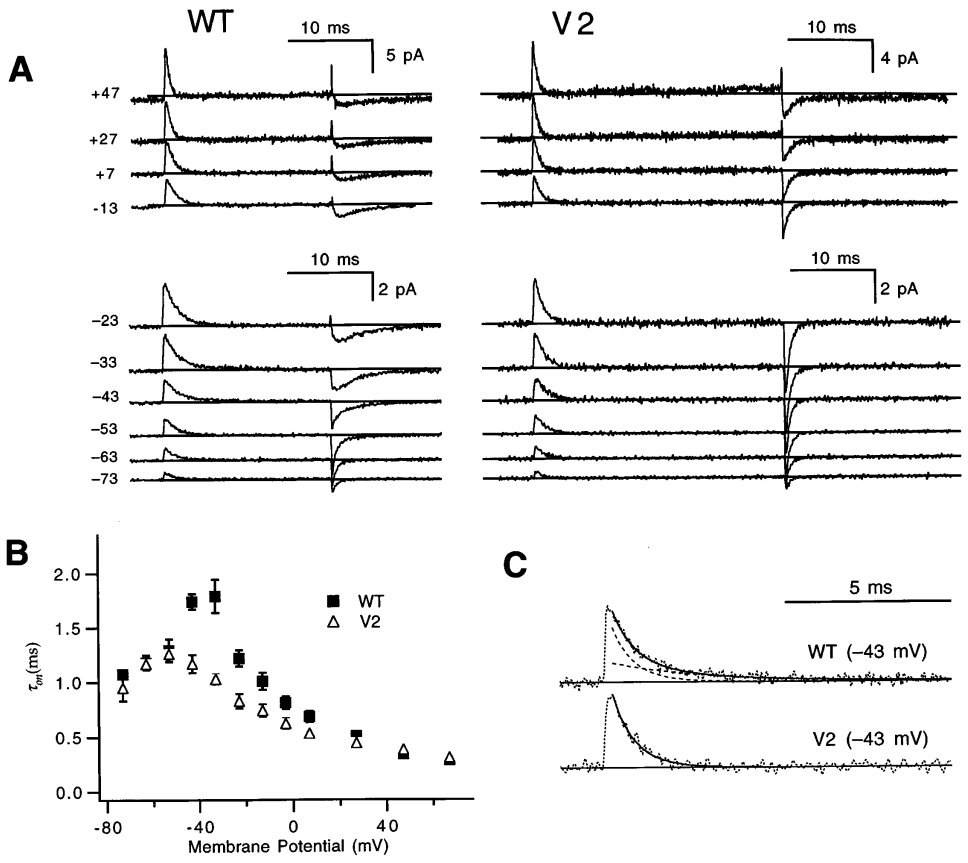

FIGURE 3. V2's effects on gating currents. (*A*) WT (*left*) and V2's (*right*) gating currents induced by voltage steps from −93 mV to test voltages between −73 and +47 mV. WT and V2 have roughly similar on current time courses at most voltages, but V2 displays markedly faster off current kinetics after the larger depolarizations. The upward deflections at the end of the test pulses at depolarized voltages reflect a leak subtraction artifact arising from charge movement that occurs during the −133- to −153-mV voltage pulse used to calculate the leak and capacitive currents (Stühmer et al., 1991). Patches w212 and v219. (*B*) The time constant τ_{on} fitted to the decay of WT and V2's on gating currents have similar values at most voltages, but are nearly two times faster at some intermediate voltages near −40 mV. Each value reflects three to seven experiments, except WT's value at +67 mV ($n = 1$). (*C*) V2's faster decaying on gating current at −43 mV in *A* reflects the absence of a slow component that is present in WT's currents, associated with WT's channel opening. WT's trace (*top*) has been fitted to a sum of two exponentials with time constants equal to 1.2 and 4.8 ms (*dashed curves*). The bottom trace shows that a scaled version of the fast component ($\tau = 1.2$ ms) accounts for V2's current very well. Horizontal lines reflect the estimated baseline of the current, taken from the mean current during the last 2 ms of the test pulse.

work that was used to assign rates for WT in the previous paper (Schoppa et al., 1998*a*), in which the gating process is approximated by a linear sequence of transitions:

$$C_0 \underset{\beta_1}{\overset{\alpha_1}{\rightleftharpoons}} C_1 \underset{\beta_d}{\overset{(\alpha_p,\,\alpha_d)}{\rightleftharpoons}} C_2 \cdots\cdots C_{N-2} \underset{\beta_{N-1}}{\overset{\alpha_N}{\rightleftharpoons}} C_{N-1} \underset{\beta_N}{\rightleftharpoons} O_N$$

(SCHEME II)

The rates shown are those that were evaluated for WT in the previous paper. To obtain values for forward rate constants, we consider mainly macroscopic ionic and gating currents obtained at depolarized voltages ($V \geq -13$ mV), where V2's charge movement is mostly complete (Fig. 1 *B*). Backward rates are mainly evaluated from macroscopic ionic and gating currents measured at hyperpolarized voltages ($V \leq -93$ mV), where little charge movement occurs.

Estimates of α_1, β_1, and α_p. For the WT channel, we were able to assign values for three rate constants associated with early and intermediate transitions (Schoppa and Sigworth, 1998*a*). The forward rate of the first transition α_1 was found to be rate limiting for channel activation at voltages near 0 mV, and estimates for α_1 were obtained from the kinetics of channel opening and gating currents. For V2, estimates of α_1 could be obtained with only a more limited analysis. V2's differential effects on the channel opening and on gating currents at voltages near 0 mV imply that the rate-limiting step to channel opening is a later transition. We assumed that the decay of V2's on currents still reflects α_1, and estimates for $\alpha_1(0) = 1{,}270\ s^{-1}$ ($n = 7$) and $q_{\alpha 1} = 0.28 \pm 0.02\ e_0$ were obtained (Fig. 4 *A*) that are similar to those obtained for WT ($\alpha_1(0) = 1{,}200\ s^{-1}$, $n = 7$, and $q_{\alpha 1} = 0.36\ e_0$). Estimates of the forward rate α_p of the transition that is rate limiting at large positive voltages for V2 were obtained from the values of the activation time constant τ_a at very large depolarizations ($V \geq +87$ mV; Fig. 4 *B*). The derived estimates for V2's $\alpha_p(0) = 1{,}400 \pm 100\ s^{-1}$ ($n = 5$) and $q_{\alpha p}(0) = 0.19 \pm 0.01\ e_0$ are similar to those obtained for WT ($\alpha_p(0) = 2{,}100\ s^{-1}$ and $q_{\alpha p}(0) = 0.17\ e_0$).

Estimates of the backward rate of the first transition β_1 were obtained from gating currents induced by voltage steps between −93 mV and more hyperpolarized voltages (Fig. 4 *C*). We assume that these voltages are

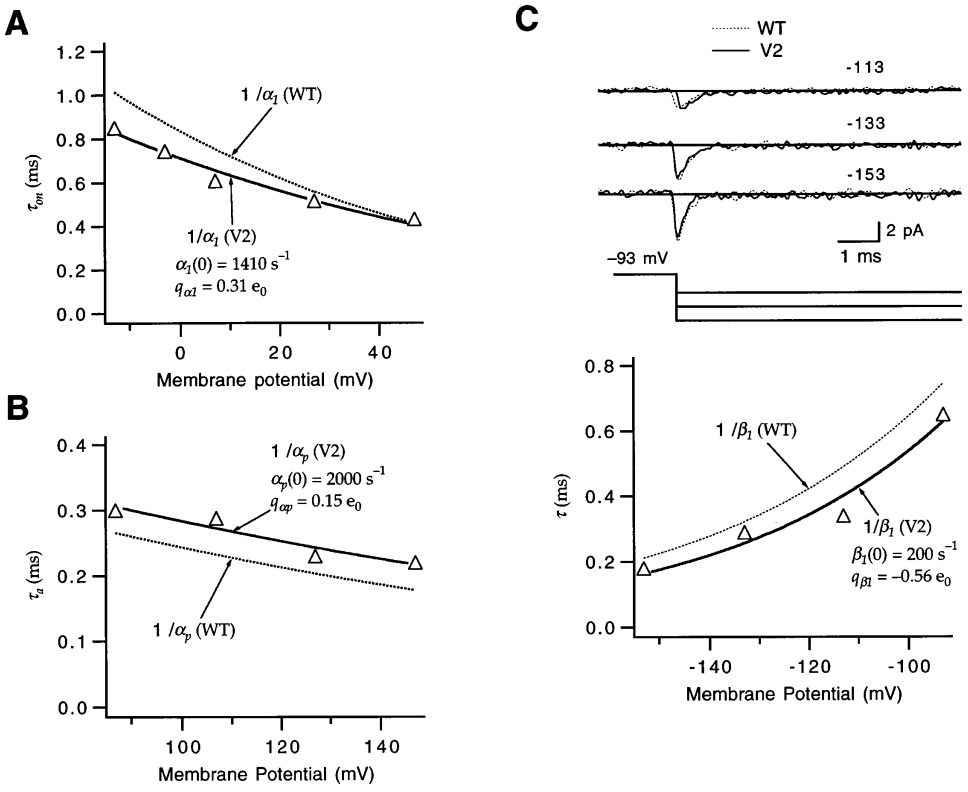

FIGURE 4. Estimates of α_1, α_p, and β_1 for V2. (*A*) The voltage dependence of α_1 was estimated by fitting an exponential to τ_{on} values derived from the on gating currents at voltages between −13 and +47 mV. From the data in the patch shown in Fig. 3 *A*, estimates were obtained $\alpha_1(0)$ = 1,410 s^{-1} and $q_{\alpha 1}$ = 0.31 e_0, which are similar to WT's (*dotted curve*). (*B*) The voltage dependence of V2's α_p was estimated by fitting an exponential to V2's τ_a values taken from macroscopic ionic current time courses measured between +87 and +147 mV. From the data in the patch shown in Fig. 2 *A*, estimates were obtained ($\alpha_p(0)$ = 2,000 s^{-1} and $q_{\alpha 1}$ = 0.15 e_0) that are similar to WT's (*dotted curve*). (*C*) The voltage dependence of β_1 was estimated from gating currents induced by voltage steps between −93 and −153 mV. These gating currents for V2 (*solid curves, top*) are nearly superimposable with WT's (*dotted curves*). Patches v240 and w249. The bottom plot shows that the time constants of the single exponentials fitted to the decay of V2's currents in this patch yielded estimates ($\beta_1(0)$ = 200 s^{-1} and $q_{\beta 1}$ = −0.56 e_0) that are similar to the mean estimates obtained for WT's β_1 (*dotted curve*).

sufficiently negative that the resulting currents reflect only charge movement in the first gating step (Schoppa and Sigworth, 1998*a*). The traces of V2's gating currents at these voltages are virtually superimposable with WT's, which is consistent with V2 having no significant effect on β_1. Indeed, the estimates of $\beta_1(0)$ = 260 ± 100 s^{-1} (n = 3) and $q_{\beta 1}$ = −0.48 ± 0.05 e_0 derived from these data are similar to those obtained for WT ($\beta_1(0)$ = 190 s^{-1} and $q_{\beta 1}$ = −0.53 e_0).

Estimate of α_N. For WT, a direct estimate of the forward rate α_N of the final transition was obtained from a rapid component in the time course of reactivation observed after very short hyperpolarizations. Fig. 5 *A* illustrates V2's reactivation time courses at +67 mV after hyperpolarizations with a fixed amplitude V_h of −93 mV, but of various durations t_h. In contrast to what was observed for WT the rising kinetics of V2's reactivation time course shows little dependence on t_h (Fig. 5, *B* and *C*). The reactivation time course for the shortest t_h = 100 μs is reasonably well accounted for by an exponential with the same time constant that is fitted to the reactivation time course for large t_h values. No fast reactivating current is observed either when V_h is changed to −13 mV (Fig. 5 *D*), which may be expected to be more effective in loading channels into closed states that are near the open state.

One explanation for the absence of a fast component in V2's reactivation time course would be that V2 slows α_N. An alternative explanation is that V2 accelerates the backward rate β_{N-1} so that the occupancy in the last closed state is never high enough for channels reactivating with the kinetics defined by α_N to be observed. We may nevertheless place a lower bound on the value of α_N from fits to the reactivation time courses in Fig. 5. There the time constant of the rate-limiting step τ_a = 0.33 ms implies that $\alpha_N \geq$ 3,000 s^{-1} at +67 mV. Using the estimate of $q_{\alpha N}$ obtained for WT, this yields $\alpha_N(0) \geq$ 1,900 s^{-1}. This lower limit is three to four times smaller than the estimate of α_N for WT ($\alpha_N(0)$ = 7,000 s^{-1}).

Estimate of β_N. The most direct estimate of WT's channel closing rate β_N was obtained from the time course of the ionic tail currents, although rather elaborate

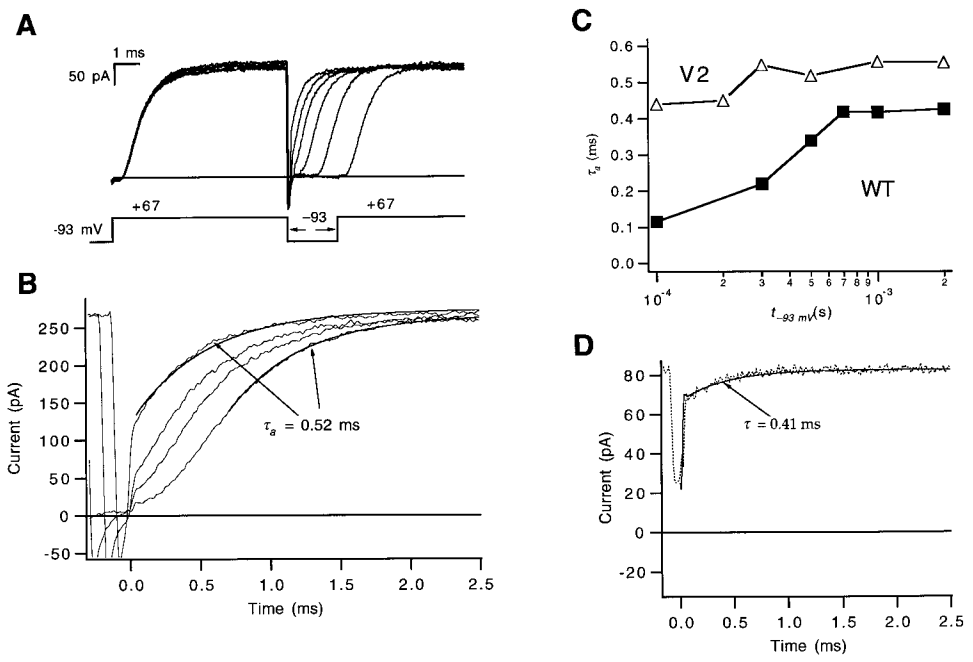

FIGURE 5. Failure to estimate α_N from V2's reactivation time courses. (*A*) V2's ionic currents elicited by a triple-pulse stimulus, using a pair of depolarizations to +67 mV separated by a voltage step to a hyperpolarized voltage V_h = −93 mV. The displayed currents correspond to hyperpolarizations of different durations t_h between 100 and 2,000 μs. Tail currents during the second pulse were inward since the pipette solution contained 5.4 mM K^+ replacing an equivalent amount of the *N*-methyl-D-glucamine$^+$ ($NMDG^+$). Data were filtered at 12 kHz. Patch v165. (*B*) No fast-reactivating component is evident in the same traces that have been expanded and time shifted to align the start of the test pulses. Only traces corresponding to t_h = 100, 200, 300, and 500 μs are shown. The current for t_h = 500 μs has been fitted to a single exponential (with τ_a = 0.52 ms), and the current for t_h = 100 μs is shown to be reasonably described by an exponential with the same time constant. (*C*) The negligible effect of prepulses of different t_h on V2's reactivation time course compares with the strong dependence for WT, reflected in the nearly fourfold decrease in the derived τ_a values for shorter t_h. Patches w448 and v165. (*D*) V2's reactivation time course at +67 mV in a different patch (v162) for V_h = −13 mV and t_h = 100 μs. To demonstrate that we have not missed a fast reactivating component that may have been obscured in the instantaneous current change, the reactivation time course has been fitted to Eq. 7 from Schoppa and Sigworth (1998*a*), which explicitly takes into account the delays in the recording system. It was assumed that the change in current due to gating is described by a function *x(t)* with a time constant (τ = 0.41 ms) that matches the τ_a value derived from V2's ionic current at +67 mV, measured in the absence of any conditioning pulses. The amplitude (−15 pA) was taken from the amount of decay of V2's tail current in the same patch at 100 μs. Data were filtered at 12 kHz.

measures were required to account for the fact that WT's channel deactivation time course at most voltages reflects multiple reopenings of the channel. Estimates for WT's β_N were obtained from fits of the sum of two exponentials to the tail currents at extremely hyperpolarized voltages (between −153 and −203 mV). V2's β_N, however, could be evaluated using a much simpler strategy.

Fig. 6 *A* illustrates traces of WT's and V2's tail currents that were measured at voltages down to −93 mV. At all voltages, V2's deactivation is much faster than WT's. When a single exponential is fitted to these currents, it is seen that the time constants τ_{tail} are not only smaller but have a weaker voltage dependence for V2 (Fig. 6 *B*). Fitting the voltage dependence of τ_{tail} results in estimates for q_{tail} of 1.1 ± 0.04 e_0 (n = 4) and 0.53 ± 0.05 e_0 (n = 5) for WT and V2, respectively. On the other hand, V2's q_{tail} nearly matches the voltage sensitivity of β_N that was estimated for WT ($q_{\beta N}$ = −0.57 e_0). The similarity between V2's q_{tail} and $q_{\beta N}$ implies that V2 changes the deactivation process from one that reflects the last two transitions to one that is a simple function of the channel closing rate β_N. Consistent with the V2's tail current time course reflecting a single transition, it is reasonably well accounted by a single exponential (Fig. 6 *A*). The τ_{tail} values at $V \leq$ −23 mV yielded an estimate for $\beta_N(0)$ = 580 ± 100 s^{-1} (n = 5), which is approximately four times larger than the estimate for WT ($\beta_N(0)$ = 150 s^{-1}).

For WT channels, estimates for the reverse rate of the second to last transition β_{N-1} were obtained by simultaneously considering the fast component in the reactivation time course that corresponds to α_N, and also the double-exponential nature of the tail currents. This analysis could not be performed on V2 since it lacks a fast component in the reactivation time course and the tail currents do not show multiple components. The assignment of V2's β_{N-1} will rely on single channel data described below.

V2's effect on α_d and β_d. While we were unable to assign values for the forward and backward rates of any other of V2's transitions from macroscopic current measurements, these data can be used to test whether V2 causes a change in the rates of these transitions. The rates of these additional transitions, which make a major contribution to the delay in activation, have been assigned the parameters α_d and β_d. As described in the preceding paper, the parameters reflect the summed properties of many intermediate transitions.

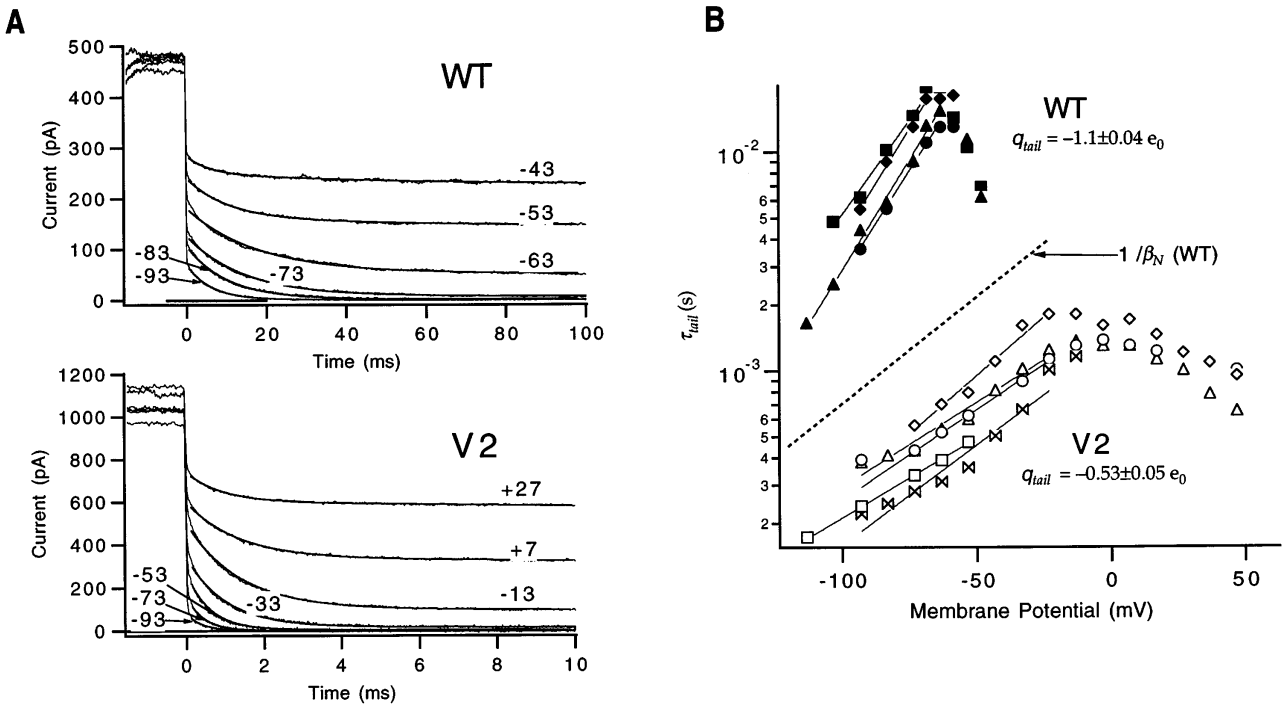

FIGURE 6. Estimate of β_N. (*A*) Across a range of test voltages, WT's tail currents decay much more rapidly than V2's (taking into account the different time scales). The tail currents were measured after prepulses to +7 and +67 mV, respectively, for WT and V2; they were outward since measurements were made with 0 mM pipette K^+. Estimates of the tail current decay time constant τ_{tail} were obtained by fitting the deactivation phase of the tail current to a single exponential. (*B*) The τ_{tail} values obtained from four WT (*closed symbols*) and five V2 (*open symbols*) patches were fitted to an exponential function of voltage yielding estimates of $\tau_{tail}(0)$ and q_{tail}. Fits were made only to the τ_{tail} values at voltages at which the time constant values become faster with increasingly negative voltages ($V \leq -63$ mV for WT and $V \leq -23$ mV for V2). For most of the patches, currents were measured in 0 mM pipette K^+, but for one patch each for WT and V2, currents were measured with 14 mM pipette K^+ (▲ and □, respectively). For comparison, the value of $1/\beta_N$ derived for WT in Schoppa and Sigworth (1998*a*) is plotted as a straight dashed line, indicating that V2's tail current decay has a similar voltage sensitivity as the channel closing rate.

Information about the effect of V2 on α_d and β_d was first obtained by comparing WT's and V2's on and off gating current time courses. While the decay of the on currents at depolarized voltages reflects the rate-limiting α_1, information about the rates of the transitions that follow α_1 resides in the time course of current near its peak. Fig. 7 *A* superimposes WT and V2 on currents that were measured at two depolarized voltages (−13 and +27 mV). The time courses match quite well, consistent with V2 having similar forward rates for all of the rapid intermediate transitions. V2's effect on reverse rates was evaluated by comparing WT's and V2's off currents. To remove the contribution of channels residing in the open state to the off current time course, which would obscure the analysis of the intermediate transitions, we compared WT's and V2's off gating currents measured after prepulses that preload channels into intermediate and late closed states but not the open state. Fig. 7 *B* compares V2's off currents after a long depolarization to −33 mV with WT's off currents measured after a 2-ms depolarization to the same voltage. These prepulses move most (~70–80%) of the charge but result in few open channels (<15% and <<1% for WT and V2, respectively). The similar off current kinetics suggests that V2 has little effect on the backward rates of virtually all of the gating transitions, apart from the final transitions.

A second measure of V2's effect on α_d and β_d was provided by a comparison of the delay in the macroscopic channel opening time course. At depolarized voltages, the delay is expected to reflect the forward rates of all but the rate-limiting step to channel opening (Schoppa and Sigworth, 1998*a*). The δ_a values for V2 (Fig. 2 *C*) are very similar to those of WT, tending however to be slightly longer (by 10–30%). The small difference in the delay is consistent with V2 having a small effect on the forward rates of a large number of transitions. A measure of β_d was obtained by analyzing the delay in V2's reactivation time course after hyperpolarizations of different voltages and of different durations t_h, using a strategy similar to that used for WT in the previous paper (Schoppa and Sigworth, 1998*a*). The resulting relationships between t_h and the delay δ_a are nearly identical for WT and V2 (data not shown), which is consistent with V2 having little effect on β_d.

V2 also had little effect in an experiment that evalu-

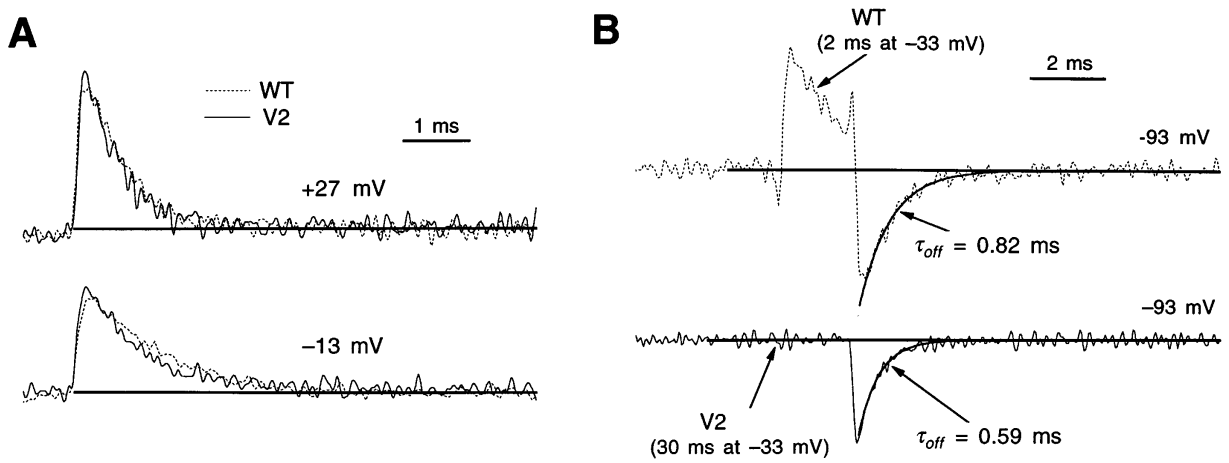

FIGURE 7. V2 has little effect on α_d and β_d gating currents. (*A*) WT (*dotted curves*) and V2 have nearly superimposable on gating currents at −13 and +27 mV, including similar time courses near the peak of the current. The current amplitudes were scaled slightly so that the peaks match. Patches w212 and v219. (*B*) Comparison of WT's and V2's off gating currents, following voltage steps that preload channels into late closed states but not the open state. For WT, the current was measured after a 2-ms pulse to −33 mV, and V2's current was measured after a 20-ms pulse to the same voltage. WT and V2's off currents have been fitted to a single exponential, yielding similar time constants τ_{off}. The slightly slower time course for WT probably reflects the contribution of the small fraction of channels that are open at that end of the prepulse, which contribute a small slow component to the off current. Patches w217 and v219.

ated the Cole-Moore delay (Cole and Moore, 1960). This experiment evaluates the effect of different amplitude prepulses on the delay in the channel opening during a subsequent test pulse. (These data are not shown here, but see Fig. 18 in Schoppa and Sigworth, 1998*b*). Since the voltage dependence of the delay reflects the equilibria of the various transitions that contribute to the delay, these results suggest, roughly, that the ratio of α_d and β_d for WT and V2 is similar.

More observations about V2's off gating currents measured after intermediate amplitude depolarizations. We report here results obtained from one additional experiment that

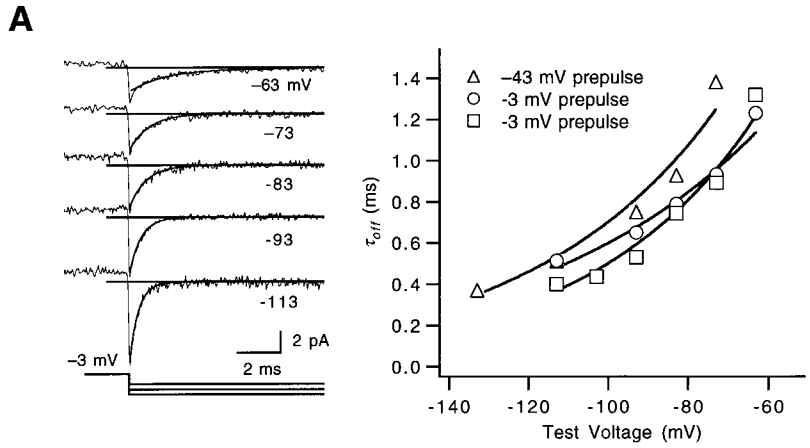

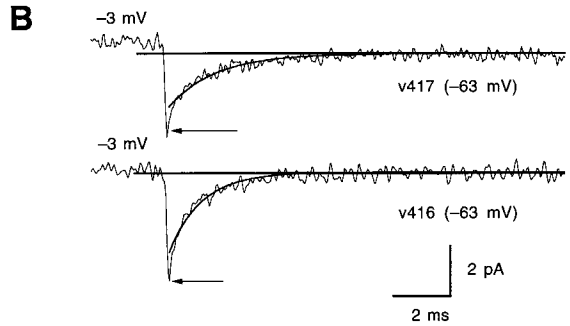

FIGURE 8. V2's off gating currents yield other information about intermediate transitions. (*A*) V2's off gating currents measured after a prepulse to −3 mV were used to estimate the partial charge $q_{\beta d}$ of the backward rates of intermediate transitions. The off currents measured at test voltages between −63 and −113 mV were fitted to an exponential, yielding a decay time constant τ_{off}. The τ_{off} values from this and two other patches were then fitted with an exponential function of voltage (*solid curves, right*), yielding values for $q_{\beta d}$ = −0.44, −0.54, and −0.61 e_0. For one of the displayed experiments, the prepulse voltage was −43 mV. (*B*) Close examination of V2's off gating current at −63 mV (from this and one other patch) indicates the presence of a fast component (*arrows*) that is poorly accounted for by a fit of a single exponential, consistent with some intermediate transitions having more rapid backward kinetics than the first transition at this voltage.

was performed for V2. Off gating currents were measured after prepulses of a fixed amplitude (−3 mV) with variable test voltages between −63 and −113 mV (Fig. 8 *A*). Since the prepulse moves most (85%) of V2's charge but opens few V2 channels (P_o = 0.2), the measured off currents should reflect the backward rates of both the first and intermediate transitions.

These currents were first used to obtain a rough estimate of the charge $q_{\beta d}$ that determines the voltage sensitivity of the backward rates of intermediate transitions. Single exponentials were fitted to these currents to estimate a decay time constant τ_{off}; the τ_{off} values were then fitted to an exponential function of voltage, yielding $q_{\beta d}$ estimates in three patches of −0.44, −0.54, and −0.61 e_0.

Single exponentials failed to fit a rapid component that is visible at some test voltages, however. The deviation is illustrated in the expanded traces of off current at −63 mV measured from two patches in Fig. 8 *B*. We take the presence of a fast component in the off current to reflect the presence of fast intermediate transitions; in the context of a sequential scheme, a fast component of the gating current must reflect the kinetics of the first transitions that occur during the relaxation. In these two patches, no fast component was observed in the off current at voltages more negative than −63 mV (data not shown), which might imply that the fast and slow components have different voltage dependences.

Analysis of Single-Channel Behavior

Additional information about V2's effects on the rates of the transitions nearest the open state was obtained from measurements of single channel currents. We begin by describing V2's single channel activity (Fig. 9 *A*). At voltages where P_o is low (−13 and −3 mV), V2 has a latency to first opening of ~10 ms, and long closures of a similar duration that separate brief (2–3-ms) bursts of channel openings are seen. During the bursts, the channel sometimes closes into short-lived closed states. With an increase in voltage, the main changes in the single channel activity are reductions in the time to first opening and the duration of the long closures (compare the traces at −13 and +7 mV). At the highest voltages (+107 mV), V2's single channels are similar to WT's (Hoshi et al., 1994; Schoppa and Sigworth, 1998*a*), opening rapidly at the beginning of the pulse and remaining open for most of the trace, closing occasionally into short-lived closed states.

The closed dwell time histograms that correspond to these data at voltages between −13 and +27 mV (Fig. 9 *B*) were well fitted by a mixture of two exponentials. With increasing voltage there is a marked reduction in the duration of the long closures, while the relative amplitude of the long closure component and the duration of short closures show less change. The closed time histograms obtained at the highest voltages (+67 and +107 mV) display the three populations of closures characteristic of WT at the same voltages (Schoppa and Sigworth, 1998*a*). At all voltages, V2's open time histograms (Fig. 9 *C*) were well fitted by a single exponential, which is consistent with a single open state (Hoshi et al., 1994).

V2's effects on transitions to C_i, C_{f1}, and C_{f2}. Single channel data from WT channels have been useful for obtaining information about states that are not in the activation path (Hoshi et al., 1994; Schoppa and Sigworth, 1998*a*). In the previous paper, we suggested that there are several such states:

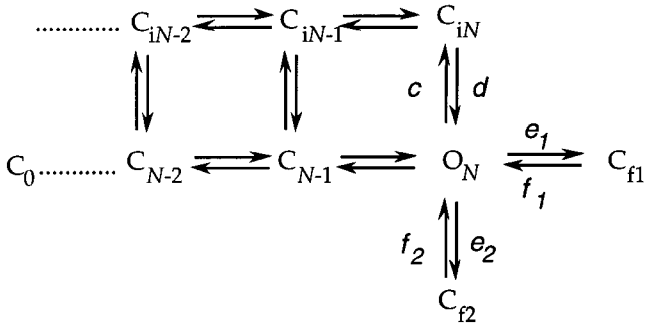

(SCHEME III)

These include the states C_{f1} and C_{f2} that correspond to the observed short duration closures at depolarized voltages, and a set of states C_i that corresponds to the observed 1–2-ms component in the closed time histograms. Apparently, the C_i states can be entered from closed states that are in the activation path as well as from the open state.

The rates d, f_1, and f_2 of the transitions from the states C_{iN}, C_{f1}, and C_{f2} to the open state are reflected in the closed time distributions at very depolarized voltages, where the open channel rarely closes into the activation path. Fig. 10 *A* superimposes the "average" WT and V2 closed time histograms at high voltages ($V \geq$ +47 mV). The shapes of the histograms cannot give direct information about rate constants, since many of the closures are poorly resolved; however, the fact that V2's average histogram matches WT's is consistent with V2 not altering the three rates.

The sum of the rates c, e_1, and e_2 of the transition from the open state to each of these three states determines the channel open time at very depolarized voltages (Fig. 10 *B*). While the poorly resolved short closures prevented a reliable estimate of the true channel open time, we could obtain an estimate of the effect that V2 has on these rates. Assuming that WT and V2 have identical closed time distributions at these voltages, an estimate of the effect of V2 on the stability of the open state may be made without correcting for missed events. At all voltages, WT's uncorrected open

times are three- to fourfold longer than V2's. This, taken together with the similar shapes of WT and V2's closed time histograms, would suggest that V2 increases each of the rates by a factor of 3–4.

Finally, to evaluate V2's effect on the transition to C_i states from closed states in the activation path, we compared the cumulative first latency histograms of WT and V2 at very depolarized voltages (Fig. 10 *C*). WT's la-

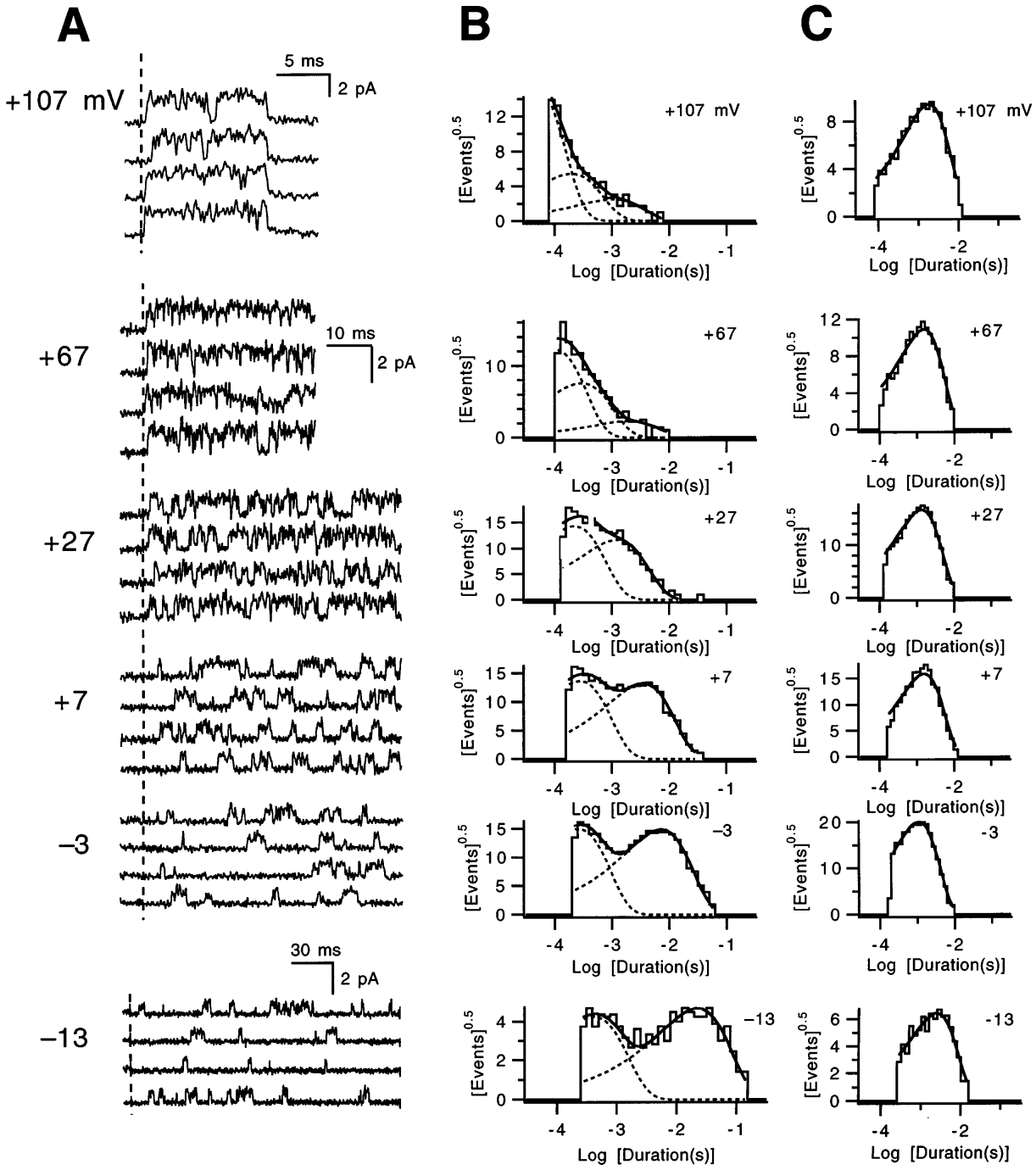

FIGURE 9. V2 single channel activity at voltages between −13 and +107 mV. (*A*) Single channel activity induced by steps from −93 mV to the indicated voltages. The data displayed at voltages between −3 and +67 mV reflect measurements in one patch (v433) and are plotted on the same scale. The data at the two extreme voltages reflect two additional patches (v428 and v344). The dashed vertical line reflects the beginning of the test pulse, and, for all but the currents at +107 mV, the currents measured after the test pulse are not shown. In our measurements, V2's single channel conductance was usually ~30% smaller than WT's (corresponding to a change in conductance from 11 to 8 pS). (*B*) Closed time histograms derived from the experiments shown in *A*. Superimposed solid curves on histograms are fits to mixtures of two or three exponentials; dashed curves illustrate each component. Each histogram contains at least 630 events. (*C*) Open time histograms, each fitted with a single exponential.

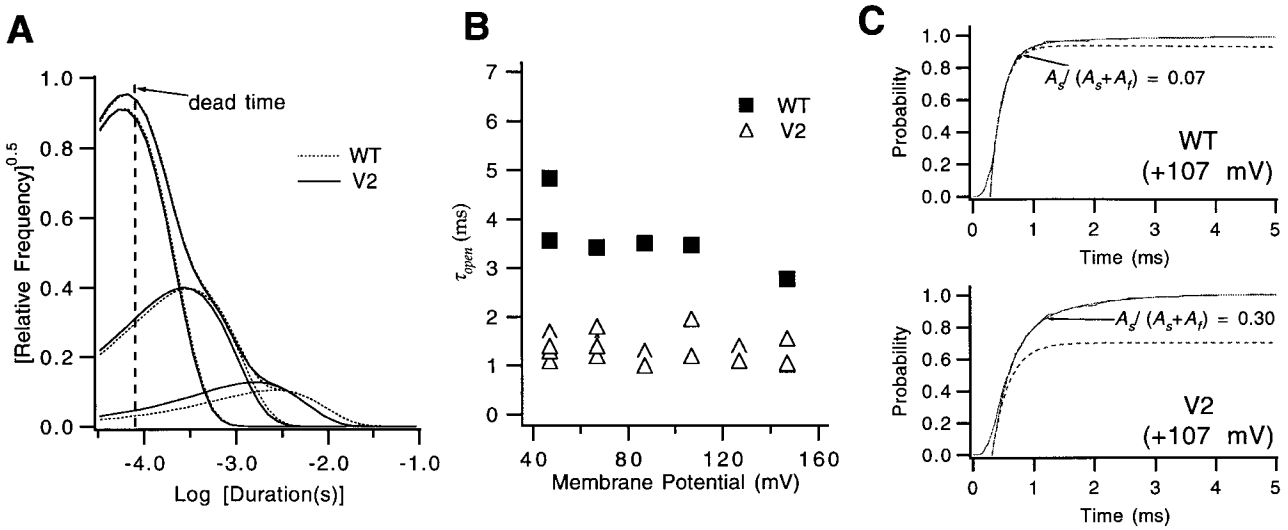

FIGURE 10. V2's effects on transitions to closed states outside of the main activation path. (*A*) WT (*dotted curves*) and V2 have nearly superimposable closed dwell-time histograms at very large depolarizations, indicating that the V2 has little effect on the transitions from C_{iN}, C_{f1}, and C_{f2} that correspond to each of the three components in these histograms. The time constants and amplitudes of the three exponentials fitted to 5 WT and 22 V2 closed time histograms at $V \geq +47$ mV were averaged, and the curves reflect the derived means. (*B*) The measured open times for V2 at large depolarizations (△) are approximately one-third as long as WT's (■), indicating that V2 destabilizes the open state relative to C_{iN}, C_{f1}, and C_{f2}. Open times are uncorrected for missed events, but may be compared since WT and V2 display the same closed time distributions at these voltages (from *A*), and the analysis filtering bandwidths were set to be equal for WT and V2. Each value reflects a single experiment. (*C*) WT (*top*) and V2 (*bottom*) cumulative first latency histograms at +107 mV were fitted to the sum of two exponentials (see legend for Fig. 2 *A*), starting at the time when $P = 0.5$. The dashed curves reflect the fast component in the same fits. The main difference between the fits for WT and V2 is the amplitude of the slow component with time constant τ_s, indicating that V2 increases the probability that a channel enters C_i states from closed states in the activation path. In the fitting, the values for τ_s for WT and V2 were 1.9 and 1.3 ms, respectively; values for the fast time constant τ_a were 0.21 and 0.29 ms. The values for A_f and A_s in the fits were adjusted for the delay in the fitted function. The two histograms reflect 182 and 258 sweeps, respectively. Patches w266 and v344.

tency histograms at $V \geq +47$ mV display a slow component that corresponds to channels entering C_i from closed states in the activation path (Schoppa and Sigworth, 1998*a*). Compared with the WT latency histogram at +107 mV, V2's histogram has a slow component approximately four times larger in amplitude; the fitted fast and slow time constants are, however, very similar. An increased amplitude slow component was also consistently observed in the macroscopic activation time course at large depolarizations ($V \geq +47$ mV), where, on average, V2's slow component accounted for 26 ± 2% of the time course ($n = 28$) compared with WT's 8 ± 1% ($n = 21$). Since it is not known from which closed states *Shaker* channels can enter C_i states, it is not clear whether the larger slow component for V2 arises from increased rates for transitions into C_i states, or simply is an effect of altered occupancies of states in the activation pathway.

Estimate of β_N and β_{N-1} from single channels. V2's single channel data could also be used to estimate the rates of the final transitions that are in the activation path. Indeed, one relevant observation has already been presented, which is V2's three- to fourfold shorter channel open times at depolarized voltages (Fig. 10 *B*). At these high voltages, most of the closures that determine the channel open time reflect closures into states that are not in the activation path, but it is notable that the magnitude of V2's effect on the open times nearly matches the fourfold faster channel closing rate into the activation path β_N that was estimated from macroscopic tail currents. The rates of channel closure into the states that are not in the activation path and β_N would all be expected to reflect the stability of the channel open state.

Other more direct information about the final transitions resides in the relatively well resolved single channel activity at V2's activation voltages (between −13 and +27 mV). The large difference in the voltage range where V2 channels open compared with the voltage range of charge movement (Fig. 1, *A* and *B*) suggests that the single channel activity at these voltages reflects the properties of just the subset of transitions that occur at high voltages. The fact that the observed long closures have a mean duration that matches the time constant fitted to the first latency histograms (Fig. 11 *A*) would indicate that these closures reflect sojourns in states in the activation path. We may, then, expect that the single channel activity reflects the rates α_N, β_N, and β_{N-1} of the last two transitions in the activation path.

The approach that will be used in this analysis is first to consider two simple schemes that could each, in principle, describe V2's single channel activity at its activation voltages. The first possibility is reflected by the reduced three-state scheme,

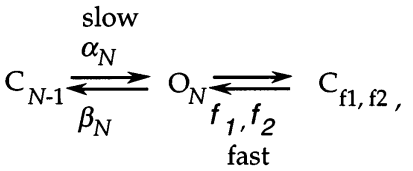

(SCHEME IV)

in which the observed short duration closures are entirely contributed by sojourns in the two closed states C_{f1} and C_{f2} that are outside of the main activation path. The long closures would reflect sojourns in late states in the activation path, here represented by the single state C_{N-1}. The observed bursts of openings would reflect the channel traversing back and forth between the open state and C_{f1} and C_{f2}, and is terminated when the channel closes into C_{N-1}. The second possibility that we consider is the four-state scheme,

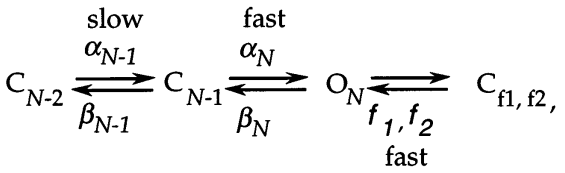

(SCHEME V)

in which the short duration closures are contributed by sojourns in the states C_{f1} and C_{f2}, as well as sojourns in C_{N-1}. The observed long closures would then reflect sojourns in closed states that are in the activation path that occur before C_{N-1}, and the bursts of openings would reflect channels traversing from the open state into C_{f1}, C_{f2}, and C_{N-1}, and are terminated when the channel closes back into C_{N-2}.

An easy way to discriminate between these two possibilities takes advantage of the reliable estimate for V2's channel closing rate β_N that has already been obtained (Fig. 6). Since, during the bursts of openings, the amount of time that the channel spends in the open state is long relative to the amount of time it spends in closed states (Fig. 9 *A*), Scheme IV predicts that the mean burst duration m_B will be equal to $1/\beta_N$. Scheme V predicts that m_B will be larger than $1/\beta_N$ by an amount that is a function of the ratio of α_N to β_{N-1}. Fig. 11 *B* compares $1/\beta_N$ with values for m_B obtained in five separate patches. This comparison indicates that these bursts apparently have the same duration as $1/\beta_N$. Fitting an exponential to the m_B values at different voltages yields estimates $m_B(0) = 1.9 \pm 0.3$ ms and $q_{mB} = 0.45 \pm 0.05$ e_0, which are nearly identical to the values of $1/\beta_N$ ($1/\beta_N(0) = 1.7$ ms and $-q_{\beta N} = 0.53$ e_0). These results imply that the bursts of openings are terminated by the channel closing into the activation path and that Scheme IV is a better representation of V2's single channel activity at these voltages.

Consideration of the sum of the rate constants indicates that Scheme IV cannot be explicitly correct. In particular, Scheme IV implies that the long closures in the single channel activity correspond to sojourns in the last closed state in the activation path C_{N-1}, but this would be incompatible with what is known about the rate α_N from macroscopic currents. The observed long closures are ten milliseconds in duration (at −3 mV), but our lower bound estimate for $\alpha_N(0)$ is 1,900 s^{-1}, which would imply that the closures that correspond to sojourns in C_{N-1} (which is given by the reciprocal of the sum of α_N and β_{N-1}) can be no longer than 0.5 ms at this voltage. We may reconcile this discrepancy by an extension of Scheme IV,

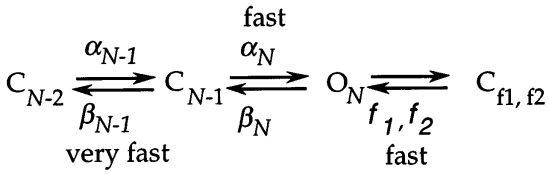

(SCHEME VI)

in which we now assume a relatively large value for α_N but an even larger value for β_{N-1}. For Scheme VI, the bursts of openings will nearly always be terminated by channel closures into the activation path since a channel that closes into C_{N-1} will more frequently proceed back into C_{N-2} or earlier closed states in the activation path rather than enter back into the open state. The long closures would arise in the absence of any rate that is very slow due to the same reason: a channel starting in earlier closed states that are in the activation path that enters into C_{N-1} will almost always proceed back into earlier closed states than enter the open state.

These results have obvious implications for estimating β_{N-1}. If we assume a value for $\alpha_N(0) = 1{,}900$ s^{-1}, the similarity in the burst duration and $1/\beta_N$ would suggest that V2's $\beta_{N-1}(0)$ is substantially larger than 1,900 s^{-1}. Some insight into the magnitude of $\beta_{N-1}(0)$ is provided by a strategy in which we compare the measured burst duration with the predictions for the bursts, assuming a model in which the bursts are determined by channel openings and closures in C_{N-1}. For this model, m_B is given by

$$m_B = \frac{1}{\beta_N}\left(1 + \frac{\alpha_N}{\beta_{N-1}}\right) + \frac{\alpha_N}{\beta_{N-1}}\left(\frac{1}{\beta_{N-1} + \alpha_N}\right). \qquad (5)$$

(Here we have neglected the effect of dwells in C_{f1} and C_{f2}, which, because they are brief and of low occu-

pancy, will have little effect on the burst duration.) In Fig. 11 *C*, a family of curves is shown superimposed on the burst length values, computed assuming the lower bound estimate of $\alpha_N(0)$ and various values for $\beta_{N\text{-}1}$. The m_B values are perhaps best described by $\beta_{N\text{-}1} = \infty$ (the curve reflecting $1/\beta_N$), but a value for $\beta_{N\text{-}1}(0)$ that is as small as 3,800 s^{-1} cannot be ruled out. Values for $\beta_{N\text{-}1}(0)$ that are smaller than 3,800 s^{-1}, however, predict a burst length that is too long. A value for $\beta_{N\text{-}1}(0) \geq$ 3,800 s^{-1} (compared with WT's $\beta_{N\text{-}1}(0) = 320$ s^{-1}) implies that the V2 mutation causes a >10-fold change in $\beta_{N\text{-}1}$.

DISCUSSION

The V2 mutation (L382V in the *Shaker* B sequence) causes a large positive shift and a reduction in the voltage sensitivity of opening of the *Shaker* potassium channel, but does not change the total gating charge (Schoppa et al., 1992). On the basis of the detailed study presented here, we find no reason to expect that this mutation causes a fundamental change in the channel activation process; instead, the mutation's effects appear to be limited to changes in a few rate constants, those governing late transitions that lead to channel opening.

Summary of V2's Effects

Besides V2's effects on the equilibrium gating properties, V2's qualitative effects on channel kinetics are (*a*) to slow channel opening at depolarized voltages, (*b*) to increase the sigmoidicity of the channel opening time course at the activation voltages, and (*c*) to make the tail currents and off gating currents decay more quickly.

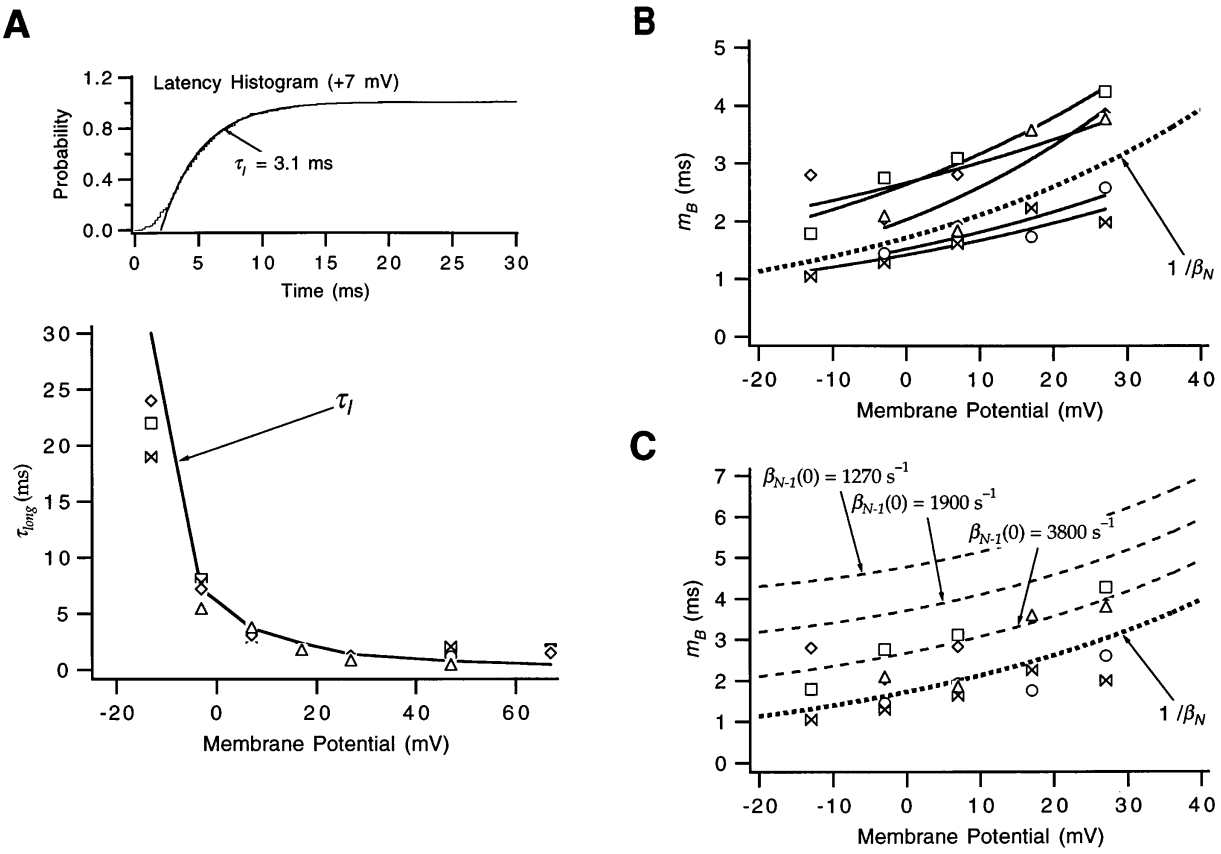

FIGURE 11. Estimates of $\beta_{N\text{-}1}$ from V2's single-channel burst durations. (*A*) V2's cumulative first latency histograms at V2's activation voltages were well-fitted by a single exponential; an example is shown at top. As shown in the plot at the bottom, the time constant τ_l of the fitted exponential is similar to the time constant τ_{long} of the longest duration exponential component in V2's closed time histograms. The τ_{long} values at $V \leq +27$ mV always reflect the longer of two fitted exponentials, and all but one of the τ_{long} values at $V \geq +47$ mV reflects the longest of three fitted exponentials. At high voltages, τ_{long} reflects closures in C_i states and is generally longer than the latency time constant. Values reflect data obtained from five patches. (*B*) The mean duration m_B of the bursts of openings separated by long closures had values similar to the reciprocal of V2's channel closing rate (*bold dotted curve*), defined by the parameters $\beta_N(0) = 580$ s^{-1} and $q_{\beta N} = -0.53$ e_0. The m_B values at $V \leq +27$ mV were calculated by normalizing the measured channel open time by the fraction of the measured closures that correspond to the longer duration exponential component in fits of the closed time histograms to the sum of two exponentials. Solid curves reflect fits of the m_B values obtained in each of the patches to an exponential, yielding estimates of $m_B(0)$ and q_{mB}. Data reflect the same experiments as in *A*. (*C*) The same m_B values as in *B* have been superimposed with the predictions of Eq. 5 for different values of $\beta_{N\text{-}1}(0)$. In the calculations, $\alpha_N(0)$ was assumed to be 1,900 s^{-1}. The charges $q_{\alpha N} = 0.18$ e_0 and $q_{\beta N\text{-}1} = -0.30$ e_0 were the WT values.

We have presented arguments that each of these differences can, at least in principle, be explained by a change in late transitions.

A more quantitative comparison of different rates indicates that V2's effects might, in fact, be limited to the final two gating transitions. Here, we have analyzed V2's currents to obtain first-pass estimates of rate constants in a way that parallels the study of WT in the previous paper. These results are summarized in Tables I and II. One marked effect is a three- to fourfold acceleration in the channel closing rate into the activation path (β_N), as evaluated from ionic tail currents. Such a magnitude of an effect on the stability of the open state was also verified from an analysis of single channel open times at depolarized voltages (reflected in the rates c, e_1, and e_2). V2 apparently has a more profound effect on the backward rate from the final closed state ($\beta_{N\text{-}1}$); this rate for V2, which is at least 10× larger than WT's, was assigned from the single channel burst durations at voltages between −13 and +27 mV. We have obtained a lower bound estimate of V2's channel opening rate α_N from V2's reactivation time course, but, in fact, we do not know if V2 actually changes this rate at all.

As far as we can tell, all of the other transitions for WT and V2 have nearly identical rates. Similar estimates were obtained for α_1, α_p, β_1, which all reflect rates of specific transitions that occur relatively early in the activation process. Similar estimates were also obtained for the parameters α_d and β_d that reflect the composite properties of all of the transitions that come between the first and last transitions. It is important to emphasize that we cannot rule out that V2 changes some of the rates that we cannot identify with our kinetic measurements. An important test of the hypothesis that V2's effects are limited to the final two transitions will be whether, in our modeling, we can account for the large family of data that we have obtained for V2 with changes in the model that are limited to the last two transitions (Schoppa and Sigworth, 1998*b*).

TABLE I

Estimates of Rate Constants for Transitions in the Activation Path

Rate at 0 mV		
WT	V2*	Partial charge
$\alpha_1(0) = 1200\ s^{-1}$	$\alpha_1(0) = 1350\ s^{-1}$	$q\alpha_1 = 0.36\ e_0$
$\alpha_p(0) = 2100\ s^{-1}$	$\alpha_p(0) = 1570\ s^{-1}$	$q\alpha_p = 0.17\ e_0$
$\alpha_N(0) = 7000\ s^{-1}$	$\alpha_N(0) \geq 1900\ s^{-1}$	$q\alpha_N = 0.18\ e_0$
—	$\alpha_d(0) = \alpha_d(0)$WT	$q\alpha_d = 0.25\ e_0$
$\beta_1(0) = 190\ s^{-1}$	$\beta_1(0) = 200\ s^{-1}$	$q\beta_1 = -0.53\ e_0$
$\beta_N(0) = 150\ s^{-1}$	$\beta_N(0) = 520\ s^{-1}$	$q\beta_N = -0.57\ e_0$
$\beta_{N\text{-}1}(0) = 320\ s^{-1}$	$\beta_{N\text{-}1}(0) \geq 3800\ s^{-1}$	$q\beta_{N-1} = -0.30\ e_0$
$\beta_d(0) = 540\ s^{-1}$	$\beta_d(0) = 540\ s^{-1}$	$q\beta_d = -0.24\ e_0$

*In some cases, the listed values for V2 differ slightly from the estimates that are given in the text (for $\alpha_1(0)$, $\alpha_p(0)$, $\beta_1(0)$, and $\beta_N(0)$). To obtain the modified estimates, we refitted selected voltage-dependent current parameters, while constraining the partial charges to be equal to the values obtained for WT in the previous paper (listed on the right).

V2 Does Not Cause a Fundamental Change in the Activation Gating Process

An underlying assumption in our comparison of activation gating in WT and V2 channels is that V2 undergoes the same conformational changes and kinetic steps as WT during its activation process. Several lines of evidence support this assumption. First, not only is the maximal charge movement equal in the two channel types (Schoppa et al., 1992; Fig. 1 *B*), but also the partial charges that determine the voltage dependence of the rate constants α_1, β_1, and β_N have been shown in the present study to be very similar in WT and V2. Second, the similarity of the delay in the activation time course (Fig. 2 *C*) suggests that the same large number of voltage-dependent transitions is operable in both channel types. Third, it should be kept in mind that the shifts in activation voltage due to amino acid substitutions at L382 correspond to only small changes $\Delta\Delta G$ in the energy to open the channel, on the order of 1 kcal/mol per *Shaker* subunit. These moderate energy changes are consistent with a simple change in the environment of this residue during activation (Sigworth, 1994; Holmgren et al., 1996). Thus, the effect of the V2 mutation can be imagined as a small perturbation of one or a few energy barriers, rather than as a wholesale remodeling of the energy landscape of the channel protein. We find no reason to reject the assumption that V2 undergoes the same conformational changes as WT in the process of activation.

Novel Insights into the Activation Gating Process from V2's Data

Several new pieces of information about the activation gating process came from V2's data. The first is derived from the shape of V2's *q-V* relation. The separation of the *q-V* relation into two components (Fig. 1, *B* and *C*) suggests that the charge movement q_H associated with a

TABLE II

Estimate of Rate Constants for Transitions to States Outside of the Activation Path

Rate at 0 mV		
WT	V2	Partial charge
$c = 5\ s^{-1}$	$c = 15\ s^{-1}$	$qc = 0.09\ e_0$
$d = 300\ s^{-1}$	$d = 300\ s^{-1}$	$qd = 0.07\ e_0$
$e_1 = 200\ s^{-1}$	$e_1 = 600\ s^{-1}$	$qe_1 \approx 0.0\ e_0$
$f_1 = 1600\ s^{-1}$	$f_1 = 1600s^{-1}$	$qf_1 = 0.20\ e_0$
$e_2 \approx 10^3\ s^{-1}$	$e_2 \approx 3000\ s^{-1}$	$qe_2 - qf_2 = 0.0\ e_0$
$f_2 \approx 10^4\ s^{-1}$	$f_2 \approx 10^4\ s^{-1}$	

subset of late gating transitions is 2 e_0 in magnitude. From our kinetic analysis of WT in the preceding paper, it is already known that the final transition has a valence of only 0.75 e_0 (the sum of $q_{\alpha N} = 0.18\ e_0$ and $q_{\beta N} = -0.57\ e_0$); thus there must be more than one transition making up this charge movement of 2 e_0. This consideration will be used in constraining the properties of the final transitions in the following paper.

We also obtained information about intermediate transitions from a set of measurements of V2's off gating currents after prepulses that were chosen to optimize the characterization of the intermediate transitions. This experiment was more easily done in V2 than in WT because the mutation causes channel opening to occur at much more positive voltages compared with the midpoint of the intermediate transitions. The observed off currents (Fig. 8) have two notable properties. The first is that the off currents decay with a voltage dependence given by the charge $q_{\beta d} \sim -0.5\ e_0$. This charge estimate roughly verifies the estimate for $q_{\beta d}$ ($q_{\beta d} = -0.24\ e_0$) obtained from the analysis of the delay in the channel reactivation time course (Schoppa and Sigworth, 1998*a*). Both of these estimates are substantially smaller than the estimates for intermediate reverse rates that have been proposed in other models (Zagotta et al., 1994*b*).

V2's off current time courses measured at −63 mV after an intermediate amplitude prepulse displayed a fast decaying component superimposed on a slow component, indicating that at least some of the intermediate transitions have rapid backward rates. Because the evidence we have provided suggests strongly that V2's effects are limited to the final transitions, we believe that it is reasonable to assume that the backward rates of WT's intermediate transitions are rapid, as they are for V2.

Original version received 3 June 1997 and accepted version received 24 November 1997.

REFERENCES

Auld, V.J., A.L. Goldin, D.S. Krafte, W. Catterall, H.A. Lester, N. Davidson, and R. Dunn. 1990. A neutral amino acid change in segment IIS4 dramatically alters the gating properties of the voltage-dependent sodium channel. *Proc. Natl. Acad. Sci. USA.* 87: 323–327.

Ayer, R.K., and F.J. Sigworth. 1997. Enhanced closed-state inactivation in a mutant Shaker K^+ channel. *J. Membr. Biol.* 157:215–230.

Bezanilla, F., E. Perozo, and E. Stefani. 1994. Gating of *Shaker* K^+ channels: II. The components of gating currents and a model of channel activation. *Biophys. J.* 66:1011–1021.

Cole, K.S., and J.W. Moore. 1960. Potassium ion current in the squid giant axon: dynamic characteristic. *Biophys. J.* 1:1–14.

Holmgren, M., M.E. Jurman, and G. Yellen. 1996. N-type inactivation and the S4-S5 region of the *Shaker* K^+ channel. *J. Gen. Physiol.* 108:195–206.

Hoshi, T., W.N. Zagotta, and R.W. Aldrich. 1990. Biophysical and molecular mechanisms of *Shaker* potassium channel inactivation. *Science.* 250:533–538.

Hoshi, T., W.N. Zagotta, and R.W. Aldrich. 1994. *Shaker* potassium channel gating. I: Transitions near the open state. *J. Gen. Physiol.* 103:249–278.

Kavanaugh, M.P., R.S. Hurst, J. Yakel, M.D. Varnum, J.P. Adelman, and R.A. North. 1992. Multiple subunits of a voltage-dependent potassium channel contribute to the binding site for tetraethylammonium. *Neuron.* 8:493–497.

Li, M., N. Unwin, K.A. Stauffer, Y.N. Jan, and L.Y. Jan. 1994. Images of purified *Shaker* potassium channels. *Curr. Biol.* 4:110–115.

Lopez, G.A., Y.N. Jan, and L.Y. Jan. 1991. Hydrophobic substitution mutations in the S4 sequence alter voltage-dependent gating in *Shaker* K^+ channels. *Neuron.* 7:327–336.

MacKinnon, R. 1991. Determination of the subunit stoichiometry of a voltage-activated potassium channel. *Nature.* 350:232–235.

McCormack, K., J.T. Campanelli, M. Ramaswami, M.K. Mathew, M.A. Tanouye, L.E. Iverson, and B. Rudy. 1989. Leucine-zipper motif update. *Nature.* 340:103.

McCormack, K., L. Lin, and F.J. Sigworth. 1993. Substitution of a hydrophobic residue alters the conformational stability of Shaker K^+ channels during gating and assembly. *Biophys. J.* 65:1740–1748.

McCormack, K., M.A. Tanouye, L.E. Iverson, J.W. Lin, M. Ramaswami, T. McCormack, J.T. Campanelli, M.K. Mathew, and B. Rudy. 1991. A role for hydrophobic residues in the voltage-dependent gating of *Shaker* K^+ channels. *Proc. Natl. Acad. Sci. USA.* 88:2931–2935.

Schoppa, N.E., K. McCormack, M.A. Tanuoye, and F.J. Sigworth. 1992. The size of gating charge in wild-type and mutant *Shaker* potassium channels. *Science.* 255:1712–1715.

Schoppa, N.E., and F.J. Sigworth. 1998*a*. Activation of *Shaker* potassium channels. I. Characterization of voltage-dependent transitions. *J. Gen. Physiol.* 111:271–294.

Schoppa, N.E., and F.J. Sigworth. 1998*b*. Activation of *Shaker* potassium channels. III. An activation gating model for wild-type and V2 mutant channels. *J. Gen. Physiol.* 111:313–342.

Sigworth, F.J. 1994. Voltage gating of ion channels. *Q. Rev. Biophys.* 27:1–40.

Stühmer, W., F. Conti, M. Stocker, O. Pongs, and S.H. Heinemann. 1991. Gating currents of inactivating and non-inactivating potassium channels expressed in *Xenopus* oocytes. *Pflügers Archiv Eur. J. Physiol.* 418:423–429.

Zagotta, W.N., T. Hoshi, and R.W. Aldrich. 1994*b*. *Shaker* potassium channel gating. III. Evaluation of kinetic models for activation. *J. Gen. Physiol.* 103:321–362.

Zagotta, W.N., T. Hoshi, J. Dittman, and R.W. Aldrich. 1994*a*. *Shaker* potassium channel gating. II. Transitions in the activation pathway. *J. Gen. Physiol.* 103:279–319.